

ESTIMATION OF LITHIUM-ION CONCENTRATIONS IN BOTH ELECTRODES OF A LITHIUM-ION BATTERY CELL

Satadru Dey
Clemson University
Greenville, SC-29607, USA
satadrd@clemson.edu

Beshah Ayalew
Clemson University
Greenville, SC-29607, USA
beshah@clemson.edu

Pierluigi Pisu
Clemson University
Greenville, SC-29607, USA
pisup@clemson.edu

ABSTRACT

For control and estimation tasks in battery management systems, the benchmark Li-ion cell electrochemical pseudo-two-dimensional (P2D) model is often reduced to the Single Particle Model (SPM). The original SPM consists of two electrodes approximated as spherical particles with spatially distributed Li-ion concentration. However, the Li-ion concentration states in these two-electrode models are known to be weakly observable from the voltage output. This has led to the prevalent use of reduced models in literature that generally approximate Li-ion concentration states in one electrode as an algebraic function of that in the other electrode. In this paper, we remove such approximations and show that the addition of the thermal model to the electrochemical SPM essentially leads to observability of the Li-ion concentration states in both electrodes from voltage and temperature measurements. Then, we propose an estimation scheme based on this SPM coupled with lumped thermal dynamics that estimates the Li-ion concentrations in both electrodes. Moreover, these Li-ion concentration estimates also enable the estimation of the cell capacity. The estimation scheme consists of a sliding mode observer cascaded with an Unscented Kalman filter (UKF). Simulation studies are included to show the effectiveness of the proposed scheme.

NOMENCLATURE

A Current collector area (cm^2)
 A_s Cell surface area exposed to surroundings (cm^2)
 a_s^\pm Specific surface area (cm^2/cm^3)

c_e Electrolyte phase Li-ion concentration (mol/cm^3)
 c_s^\pm Solid phase Li-ion concentration (mol/cm^3)
 $c_{s,e}^\pm$ Solid-phase Li-ion surface-concentration (mol/cm^3)
 $c_{s,max}^\pm$ Solid-phase Li-ion max. concentration (mol/cm^3)
 D_s^\pm Diffusion coefficient in solid phase (cm^2/s)
 $D_{s,ref}^\pm$ Diffusion coefficient at T_{ref} (cm^2/s)
 E_K^\pm Activation Energy of diffusion coefficient (J/mol)
 E_{Ds}^\pm Activation Energy of reaction rate constant (J/mol)
 E_R Activation Energy of reaction rate constant (J/mol)
 h Heat transfer coefficient of the cell ($\text{W}/\text{cm}^2\text{-K}$)
 F Faraday's constant (C/mol)
 I Current (A)
 K^\pm Reaction rate constant ($\text{cm}^{2.5}/\text{mol}^{0.5}/\text{s}$)
 K_{ref}^\pm Reaction rate constant at T_{ref} ($\text{cm}^{2.5}/\text{mol}^{0.5}/\text{s}$)
 L^\pm Length of the cell (cm)
 r Radial coordinate (cm)
 R Radius of solid active particle (cm)
 \bar{R} Universal Gas Constant ($\text{J}/\text{mol-K}$)
 $R_{f,ref}$ Contact film resistance (Ω)
 T Temperature (K)
 T_{ref} Reference temperature (K)
 T_∞ Temperature of cooling fluid (K)
 U^\pm Open circuit potential (V)
 α^\pm Charge transfer coefficient
 ρ Cell density (g/cm^3)
 v Cell volume (cm^3)
 C_p Specific heat capacity ($\text{J}/\text{g-K}$)
Superscript
 \pm positive/negative electrode

INTRODUCTION

Advanced Battery Management System (BMS) is a crucial part of Lithium-ion (Li-ion) battery technology. Apart from enabling efficient and optimal usage of the Li-ion batteries, BMS also ensures safe and reliable operation. To facilitate these functionalities, BMS depends on internal information of the Li-ion batteries such as State-of-Charge (SOC) and State of Health (SOH). As these quantities are not measured in real-time, mathematical models that capture this information are extensively used in the BMS. Several types of Li-ion battery models are presented in the literature such as: 1) Data-driven models [1],[2], 2) Equivalent Circuit Models [3],[4], and 3) Electrochemical models. Among these, electrochemical models, which are derived from the principles of electrochemistry, are argued to provide the most detailed physically interpretable, and likely accurate, information [5].

The benchmark Li-ion battery cell electrochemical model is the pseudo two-dimensional (P2D) model, which consists of nonlinear-coupled partial differential equations (PDE) [6]. However, P2D models possess high computation burden for real-time implementation and the mathematical structure is too complex for estimator design. To resolve this issue, researchers have proposed different model reductions [7], [8]. The Single Particle Model (SPM) is one of the widely used reduced models where the two electrodes are approximated as spherical particles [9], [10].

SPM model-based estimators predict the SOC of the battery cell by computing the *distributed* Lithium concentration inside the electrode using only the available real time measurements of differential voltage, boundary current and temperature. Several SPM-based estimation approaches have been presented in the literature. For example, a back-stepping PDE estimator [11], extended Kalman filter (EKF) [9], [10] are used for SOC estimation. The authors of the present paper also proposed nonlinear observers [12],[13] for SOC estimation. Another branch of work extended the SPM-based estimation by proposing adaptive SOC estimation accounting for parametric uncertainties. These include Particle Filter (PF) [14], unscented Kalman Filter (UKF) [15], Iterative EKF (IEKF) [16], adaptive PDE observer [17] and nonlinear geometric observer [18]. In this line of work, the authors of the present paper also designed sliding mode observer [19], nonlinear adaptive observer [20] for adaptive SOC estimation.

One challenge in SPM-based estimation arises from the observability problem. Lithium concentration states of the SPM with two electrodes are weakly observable from the differential voltage measurement alone [10]. This is due to the fact that the Li-ion concentration information of the individual electrodes are coupled in the differential voltage expression via their respective open-circuit potentials, whereas these states are decoupled in their state dynamics equation. Most of the estimation schemes reviewed above took the following approach: approximate one electrode's Li-ion concentration in terms of some algebraic function of another electrode's Li-ion

concentration to improve the observability [10],[11],[12]. This reduces the dynamics to a one-electrode SPM whose Li-ion concentration states are strongly observable. However, this approximation is generally built on the underlying assumption of the conservation of the total number of Li-ions in the cell.

The main contribution of this paper is that we relax the aforementioned assumption and design an estimation scheme based on the two-electrode SPM without any such approximations. The novel idea in this paper lies in the design of an estimation scheme which is able to estimate Li-ion concentration in both the positive and the negative electrodes based on an electrochemical-thermal cell model and the available real-time measurements of differential voltage, temperature and current. The advantages of having the estimates of Li-ion concentration in each electrode are: 1) It can be used to compute the capacity of the cell in real-time, 2) It will provide the SOC in each electrode that enables monitoring of the internal condition and health of the individual electrodes.

The improvement on the two-electrode SPM observability arises from exploiting the coupling between the electrochemical and thermal dynamics of the Li-ion cell [21]. The coupling from thermal to electrochemical is via the dependence of some of the electrochemical parameters and the nonlinear output voltage on the temperature. The coupling from electrochemical to the thermal is the contribution of Li-ion concentrations of the individual electrodes to the heat generation term. We use the thermal model and the temperature measurement to estimate this heat generation term that possesses additional information about the Li-ion concentrations of both electrodes. It is shown here that adding the thermal dynamics essentially leads to the observability of both the positive and negative electrode concentrations from the available measurements of voltage and cell temperature.

The structure of the estimation scheme proposed in this paper consists of two cascaded observers, Observer I and Observer II. Observer I is a thermal dynamics-based sliding mode observer that estimates a part of the heat generation term that possesses Li-ion concentration information of the electrodes. Then this estimate serves as a *pseudo-measurement* to Observer II, which is based on the two-electrode SPM. Using this *pseudo-measurement* from Observer I and the differential voltage measurement from the cell, Observer II estimates the Li-ion concentration in both the positive and negative electrodes. Observer II is designed based on Unscented Kalman filter (UKF) approach to account for the model nonlinearity.

The rest of the paper is organized as follows. In the next section, we describe the SPM and thermal modeling approach for Li-ion cell. Then we analyze the observability of the system. After that details of the estimation scheme is discussed. Then, simulation results are provided and the conclusions of the work are summarized.

MODELING OF LITHIUM-ION CELL

The Single Particle Model (SPM) is derived from the pseudo two-dimensional (P2D) electrochemical model which is a benchmark model for Li-ion cell [6]. Here, we briefly discuss the SPM [9], [10], with the schematic given in Fig. 1.

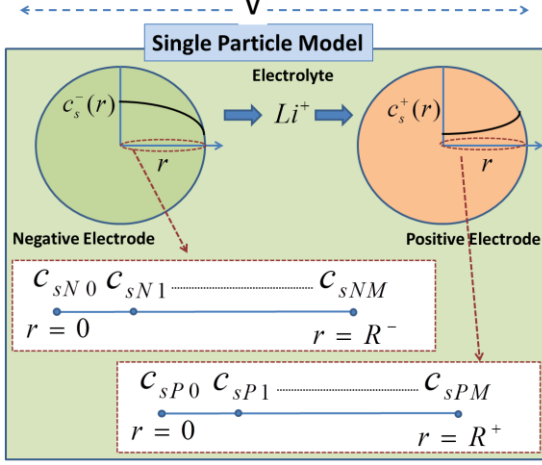


Figure 1. Schematic of the single particle model (SPM)

The SPM is obtained by approximating the cell electrodes as spherical particles under volume-averaging assumptions. This boils down to two linear PDEs describing the Li-ion diffusion in two electrode particles as given below:

$$\begin{aligned} \frac{\partial c_s^\pm}{\partial t} &= \frac{D_s^\pm(T)}{r^2} \frac{\partial}{\partial r} \left(r^2 \frac{\partial c_s^\pm}{\partial r} \right) \\ \frac{\partial c_s^\pm}{\partial r} \Big|_{r=0} &= 0, \quad \frac{\partial c_s^\pm}{\partial r} \Big|_{r=R^\pm} = \frac{\pm I}{a_s^\pm F D_s^\pm(T) A L^\pm} \end{aligned} \quad (1)$$

where c_s^\pm is the Li-ion concentration of the positive and negative electrode, D_s^\pm is the solid material diffusion coefficient of positive/negative electrode, T is the cell temperature, r is the radial axis of the particles, R^\pm is the radius of the electrode particles, F is Faraday's constant, L^\pm is the length of the positive/negative electrode and I is the charge/discharge current. The specific surface area can be computed as $a_s^\pm = 3\varepsilon_s^\pm/R^\pm$. The output voltage map is given by:

$$\begin{aligned} V &= \frac{\bar{R}T}{\alpha^+ F} \sinh^{-1} \left(\frac{I}{2a_s^+ A L^+ i_0^+} \right) \\ &- \frac{\bar{R}T}{\alpha^- F} \sinh^{-1} \left(\frac{I}{2a_s^- A L^- i_0^-} \right) + U^+(c_{s,e}^+, T) \\ &- U^-(c_{s,e}^-, T) - R_f(T)I \end{aligned} \quad (2)$$

where i_0^\pm are the exchange current densities given by:

$$i_0^\pm = k_0^\pm(T) \sqrt{c_e c_{s,e}^\pm (c_{s,max}^\pm - c_{s,e}^\pm)} \quad (3)$$

The following lumped thermal model [21] is adopted:

$$\begin{aligned} m C_p \frac{dT}{dt} &= I \left(U^+(c_{s,e}^+, T) - U^-(c_{s,e}^-, T) - V \right. \\ &\quad \left. - T \left(\frac{\partial U^+}{\partial T} - \frac{\partial U^-}{\partial T} \right) \right) - h A_s (T - T_\infty) \end{aligned} \quad (4)$$

where T is the temperature and $\frac{\partial U^\pm}{\partial T}$ are functions of $c_{s,e}^\pm$ [21], $m = \rho v$. Note that the temperature affects the open circuit potential, and the over-potential terms are functions of temperature in (2) whereas U^\pm and $\frac{\partial U^\pm}{\partial T}$ contributes to the heat generation in (4). Moreover, in this study, we assume that the solid phase diffusion coefficients (D_s^\pm), the contact film resistance (R_f) and the reaction rate constants (k_0^\pm) show Arrhenius dependence on temperature [21]:

$$\begin{aligned} k_0^\pm(T) &= k_{0,ref}^\pm \exp \left(\frac{E_K^\pm}{R} \left(\frac{1}{T} - \frac{1}{T_{ref}} \right) \right) \\ D_s^\pm(T) &= D_{s,ref}^\pm \exp \left(\frac{E_{D_s}^\pm}{R} \left(\frac{1}{T} - \frac{1}{T_{ref}} \right) \right) \\ R_f(T) &= R_{f,ref} \exp \left(\frac{E_R}{R} \left(\frac{1}{T} - \frac{1}{T_{ref}} \right) \right) \end{aligned} \quad (5)$$

where T_{ref} is the reference temperature, $k_{0,ref}^\pm$, $D_{s,ref}^\pm$ and $R_{f,ref}$ are the parameter values at that reference temperature T_{ref} .

Note: Some authors, e.g. [22] and [23] have extended the SPM and the lumped thermal model, respectively, to improve their respective predictive ability. In this work, we use the above conventional SPM along with the averaged thermal model since our objective is to illustrate the observability and estimation concept for the two-electrode SPM. Future extension of this work could consider the cited extended models.

To approximate the PDEs in (1), the spatial derivatives are discretized using finite central difference methods. This leads to a set of ODEs that will be used to form the finite dimensional state-space model. The spatial domain is discretized into $(M+1)$ nodes for both PDEs (refer to Fig. 1). The positive and negative electrodes' Li-ion concentration states at the nodes are given as: $[c_{sP0}, c_{sP1}, \dots, c_{sPM}]$ and $[c_{sN0}, c_{sN1}, \dots, c_{sNM}]$. The resulting ODEs are given in (6)-(7). We refer this as simplified SPM.

Negative electrode:

$$\begin{aligned} \dot{c}_{sN0} &= -3a_N c_{sN0} + 3a_N c_{sN1} \\ \dot{c}_{sNm} &= \left(1 - \frac{1}{m} \right) a_N c_{sN(m-1)} - 2a_N c_{sNm} \\ &\quad + \left(1 + \frac{1}{m} \right) a_N c_{sN(m+1)} \\ \dot{c}_{sNM} &= \left(1 - \frac{1}{M} \right) a_N c_{sN(M-1)} - \left(1 - \frac{1}{M} \right) a_N c_{sNM} \\ &\quad - \left(1 + \frac{1}{M} \right) b_N I \end{aligned} \quad (6)$$

Positive electrode:

$$\begin{aligned} \dot{c}_{sP0} &= -3a_P c_{sP0} + 3a_N c_{sP1} \\ \dot{c}_{sPm} &= \left(1 - \frac{1}{m}\right) a_P c_{sP(m-1)} - 2a_P c_{sPm} \\ &\quad + \left(1 + \frac{1}{m}\right) a_P c_{sP(m+1)} \\ \dot{c}_{sPM} &= \left(1 - \frac{1}{M}\right) a_P c_{sP(M-1)} - \left(1 - \frac{1}{M}\right) a_P c_{sPM} \\ &\quad - \left(1 + \frac{1}{M}\right) b_P I \end{aligned} \quad (7)$$

with $m = 1, \dots, (M-1)$, discretization steps $\Delta_N = R^-/M$, $\Delta_P = R^+/M$, $a_N = D_s^-(T)/\Delta_N^2$, $a_P = D_s^+(T)/\Delta_P^2$, $b_N = 1/a_s^- F \Delta_N A L^-$, $b_P = 1/a_s^+ F \Delta_P A L^+$.

The output voltage equation can be formed from (2) by substituting $c_{s,e}^- = c_{sNM}$ and $c_{s,e}^+ = c_{sPM}$:

$$\begin{aligned} V &= \frac{\bar{R}T}{\alpha^+ F} \sinh^{-1} \left(\frac{I}{2a_s^+ A L^+ i_0^+} \right) \\ &\quad - \frac{\bar{R}T}{\alpha^- F} \sinh^{-1} \left(\frac{I}{2a_s^- A L^- i_0^-} \right) \\ &\quad + U^+(c_{sPM}, T) - U^-(c_{sNM}, T) - R_f(T)I \end{aligned} \quad (8)$$

where i_0^\pm are the exchange current densities given by:

$$\begin{aligned} i_0^+ &= k_0^+(T) \sqrt{c_e c_{sPM} (c_{s,max}^- - c_{sPM})} \\ i_0^- &= k_0^-(T) \sqrt{c_e c_{sNM} (c_{s,max}^- - c_{sNM})} \end{aligned} \quad (9)$$

OBSERVABILITY ANALYSIS

Observability of Li-ion Concentrations of both Electrodes from only Voltage Output (Conventional SPM):

In this section, we will discuss the observability of the conventional SPM, that is the observability of the Li-ion concentration states, from only voltage output. The Li-ion concentration dynamics along with the nonlinear voltage map can be written in the state-space form:

$$\begin{aligned} \begin{bmatrix} \dot{x}_P \\ \dot{x}_N \end{bmatrix} &= \begin{bmatrix} A_P & 0_M \\ 0_M & A_N \end{bmatrix} \begin{bmatrix} x_P \\ x_N \end{bmatrix} + \begin{bmatrix} B_P \\ B_N \end{bmatrix} u \\ y_V &= U_P(x_{PM}, T) - U_N(x_{NM}, T) + n_P(x_{PM}, T) \\ &\quad - n_N(x_{NM}, T) - R_f(T)u \end{aligned} \quad (10)$$

where $x_P = [c_{sP1}, \dots, c_{sPM}]^T \in R^M$ and $x_N = [c_{sN1}, \dots, c_{sNM}]^T \in R^M$ are the Li-ion concentration states in the positive and the negative electrode, respectively, $u \in R$ is the input current, $y_V = V \in R$ is the output voltage, $x_{PM} = c_{sPM} \in R$ and $x_{NM} = c_{sNM} \in R$ are the surface concentration states of the positive and the negative electrode, respectively, $A_P \in R^{M \times M}$ and $A_N \in R^{M \times M}$ are temperature dependent tri-diagonal matrices obtained from the state matrices in (6) and (7) respectively, $0_M \in R^{M \times M}$ is the zero matrix, $B_P \in R^{M \times 1}$ and $B_N \in R^{M \times 1}$ are the input matrices derived from (6) and (7)

respectively, $U_P = U^+: R^2 \rightarrow R$ and $U_N = U^-: R^2 \rightarrow R$ are the temperature dependent open-circuit potential maps for the positive and negative electrode, respectively, $R_f \in R$ is the temperature dependent scalar film resistance, $n_P: R^2 \rightarrow R$ and $n_N: R^2 \rightarrow R$ are the first two scalar over-potential terms in (8), respectively.

Now, the observability of the system (10) can be analyzed for a given temperature $T = T^*$. Note that, the assumption of constant temperature while analyzing the Li-ion concentration dynamics makes is justified due to the fact that the temperature dynamics is much slower than the Li-ion concentration dynamics. For a given temperature $T = T^*$, the system (10) consists of a linear dynamics with a nonlinear output map. The observability can be verified using the sufficient rank condition for the local nonlinear observability notion described in [24]. To this end, the rank of the following observability matrix is checked at different operating points in the state-space for the admissible input range.

$$O(x^*, u^*) = \begin{bmatrix} \frac{\partial}{\partial x} (L_f^0[h]) \\ \vdots \\ \frac{\partial}{\partial x} (L_f^{2M-1}[h]) \end{bmatrix}_{x=x^*, u=u^*} \quad (11)$$

where $h = y_V$ represents the output voltage map, $x = [x_P^T, x_N^T]^T$ represents the state vector and u represents the input current. It is observed that the system states in (10) are unobservable according to this local observability notion. This fact was also verified in [10].

This unobservability also makes sense from the physical viewpoint considering the system (10). Note that, there is no coupling between the positive and negative electrode concentration states in the state dynamics equation in (10) i.e. A_P and A_N are not coupled. In the nonlinear output voltage map y_V , the information of positive and negative electrode surface concentrations x_{PM} and x_{NM} are coupled. Therefore, given the voltage map (where both electrode's concentration information appears) and the electrode state-dynamics represented by the A matrix in (10) (where the two electrodes states are not coupled), the states are not fully observable from the output.

Remark 1: The observability of (10) and hence the rank of (11) depends on the functions U_P and U_N which are specific to different Li-ion battery chemistries. For this analysis, we considered LiCoO₂-Graphite cells. Similar analysis can be performed on other chemistries.

To get an observable model, the negative electrode concentration is approximated as an algebraic function of the positive electrode concentration using the stoichiometry ratios of the electrodes as in [10]. While in [11], the positive electrode concentration is approximated as a function of the negative electrode concentration assuming conservation of the number of Li-ions in the cell. In this paper, we take a different approach

where we add the thermal dynamics to the two-electrode model (10), which leads to the observability of both electrode states from the measured voltage and temperature.

Observability of Li-ion Concentrations of both Electrodes from Voltage and Temperature Output (Conventional SPM with Thermal Dynamics):

In this section, we will consider the conventional SPM along with the thermal dynamics as given below:

$$\begin{aligned}
 \begin{bmatrix} \dot{x}_P \\ \dot{x}_N \end{bmatrix} &= \begin{bmatrix} A_P & 0_M \\ 0_M & A_N \end{bmatrix} \begin{bmatrix} x_P \\ x_N \end{bmatrix} + \begin{bmatrix} B_P \\ B_N \end{bmatrix} u \\
 mC_p \dot{T} &= u \{ U_P(x_{PM}, T) - U_N(x_{NM}, T) - y_V \} \\
 &\quad - uT \{ U_P^D(x_{PM}) - U_N^D(x_{NM}) \} - hA_s(T - T_\infty) \\
 y_V &= U_P(x_{PM}, T) - U_N(x_{NM}, T) + n_p(x_{PM}, T) \\
 &\quad - n_n(x_{NM}, T) - R_f(T)u \\
 y_T &= T
 \end{aligned} \tag{12}$$

where $U_P^D = \frac{\partial U^+}{\partial T} : R \rightarrow R$ and $U_N^D = \frac{\partial U^-}{\partial T} : R \rightarrow R$ are functions of x_{PM} and x_{NM} respectively and $y_T = T \in R$ is the measured temperature. In this previous section, we have seen that both electrode states are not observable from only the voltage output. However, if we consider the coupled electrochemical-thermal dynamics given in (12), it is evident that the thermal dynamics carry additional information of the electrode surface concentrations in the form of $\{U_P^D(x_{PM}) - U_N^D(x_{NM})\}$. This is the key observation we use in this paper for improving the observability of both electrode states.

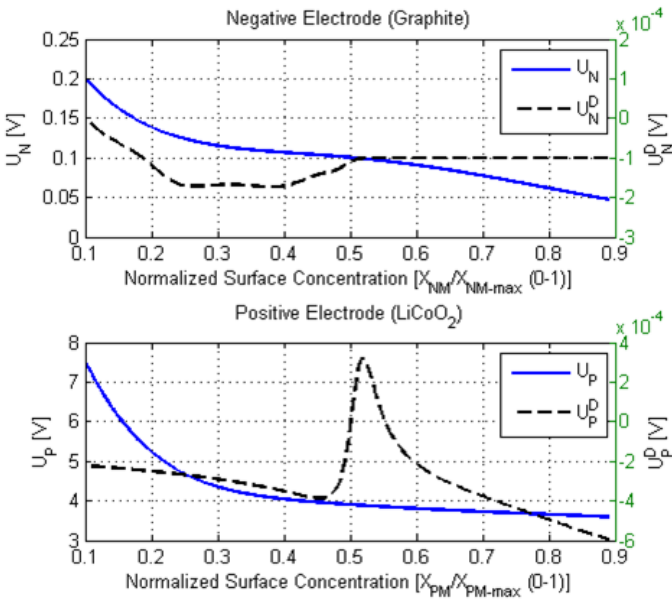


Figure 2: The functions U_P , U_N , U_P^D and U_N^D for LiCoO₂-Graphite chemistry [21]

Next we check of the observability of the system (12) at different operating points using the sufficient rank condition of the observability matrix (11) with $h = [y_V \ y_T]^T$. As stated

before, the observability of (12) depends on the functions U_P , U_N , U_P^D and U_N^D which are specific to different Li-ion battery chemistries. Here, we consider the LiCoO₂-Graphite chemistry for illustration. The functions U_P , U_N , U_P^D and U_N^D for this chemistry are shown in Fig. 2. The rank of the observability matrix O in (11) is checked at different operating points from which it is noted that the system (12) is observable at all tested operating points. However, it can be noted that the necessary condition for observability is $u^* \neq 0$. This is evident from the expression of the thermal dynamics in (12). With $u = 0$, thermal dynamics does not carry any information of the Li-ion concentration states. Hence, the system loses its observability.

ESTIMATION SCHEME

In this section, the estimation scheme is discussed in detail. The schematic of the estimation scheme is shown in Fig. 3. The scheme consists of two observers working in a cascaded manner. Observer I, which is designed based on the thermal dynamics of the system, estimates a pseudo-measurement (y_{pseudo}) signal using the current and temperature measurement. This y_{pseudo} essentially is the part in the thermal dynamics that contains the Li-ion concentration information. Observer II, which is designed based on Li-ion concentration dynamics, estimates Li-ion concentration in the positive and negative electrodes using the measured voltage and the pseudo measurement signal from Observer I. Essentially, Observer I extracts the Li-ion concentration information from the thermal dynamics which in turn acts as an added measurement to Observer II thereby improving the observability.

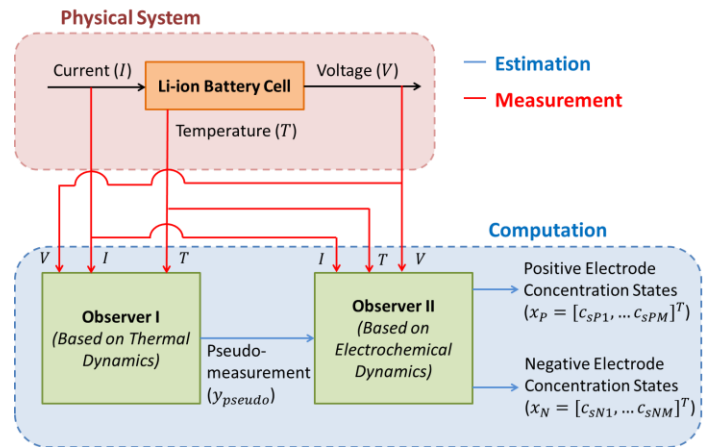


Figure 3: Estimation Scheme

Observer I

Observer I is designed using sliding mode theory [25]. The observer structure is chosen as:

$$mC_p \hat{T} = -u y_V - hA_s(\hat{T} - T_\infty) + L_T \text{sgn}(T - \hat{T}) \tag{13}$$

where y_V and T are the measured voltage and temperature. Subtracting (13) from the thermal dynamics in (12), the observer error dynamics can be written as:

$$mC_p \dot{\tilde{T}} = u\{U_P(x_{PM}, T) - U_N(x_{NM}, T)\} - uT\{U_P^D(x_{PM}) - U_N^D(x_{NM})\} - hA_s(\tilde{T}) - L_T \text{sgn}(\tilde{T}) \quad (14)$$

where $\tilde{T} = T - \hat{T}$ is the estimation error. The observer error dynamics can be analyzed by choosing the Lyapunov function candidate $V_T = 0.5mC_p \tilde{T}^2$. Taking the derivative of the Lyapunov function candidate:

$$\begin{aligned} \dot{V}_T &= mC_p \tilde{T} \dot{\tilde{T}} = [u\{U_P(x_{PM}, T) - U_N(x_{NM}, T)\} \\ &\quad - uT\{U_P^D(x_{PM}) - U_N^D(x_{NM})\}] \tilde{T} \\ &\quad - hA_s \tilde{T}^2 - L_T \tilde{T} \text{sgn}(\tilde{T}) \\ \Rightarrow \dot{V}_T &\leq |\tilde{T}| \left\{ |u| |U_P(x_{PM}, T) - U_N(x_{NM}, T)| \right. \\ &\quad \left. + |u| |T| |U_P^D(x_{PM}) - U_N^D(x_{NM})| \right. \\ &\quad \left. - L_T \right\} \end{aligned} \quad (15)$$

For a high value of the observer gain $L_T > F_{max} \triangleq |u|_{max} |U_P(x_{PM}, T) - U_N(x_{NM}, T)|_{max} + |u|_{max} |T|_{max} |U_P^D(x_{PM}) - U_N^D(x_{NM})|_{max} > 0 \forall t$, then $\dot{V}_T < 0$. The values $|u|_{max}$ and $|T|_{max}$ can be determined apriori based on the reasonable maximum input current and maximum possible temperature range for the battery operation. The values $|U_P(x_{PM}, T) - U_N(x_{NM}, T)|_{max}$ and $|U_P^D(x_{PM}) - U_N^D(x_{NM})|_{max}$ can be determined apriori based on the particular electrode chemistries. Therefore, V_T and hence the estimation error $|\tilde{T}|$ will converge to the sliding surface $s_T = \tilde{T} = 0$ in finite time as given below:

$$\begin{aligned} \dot{V}_T &\leq -\beta \sqrt{V_T}, \text{ with } \beta = (L_T - F_{max}) > 0 \\ \Rightarrow V_T &< \left(-\frac{\beta}{2} t + \sqrt{V_T(t=0)} \right)^2 \end{aligned} \quad (16)$$

The finite time can be given as $t_f \leq 2\sqrt{V_T(t=0)}/\beta$. At the sliding surface, the following conditions are true: $s_T = \tilde{T} = 0$ and $\dot{s}_T = \dot{\tilde{T}} = 0$ [25]. Using these conditions, the observer error dynamics (14) on the sliding surface can be re-written as:

$$\begin{aligned} 0 &= u\{U_P(x_{PM}, T) - U_N(x_{NM}, T)\} \\ &\quad - uT\{U_P^D(x_{PM}) - U_N^D(x_{NM})\} - v_T \end{aligned} \quad (17)$$

where v_T is the equivalent output error injection signal required to maintain the sliding motion. It is a continuous approximation of the switching signal $L_T \text{sgn}(\tilde{T})$. For real-time implementation, v_T can be extracted by passing the switching signal $L_T \text{sgn}(\tilde{T})$ through a low-pass filter [25]. Therefore, from (17) the pseudo-measurement signal can be extracted as:

$$y_{pseudo} = v_T = u\{U_P(x_{PM}, T) - U_N(x_{NM}, T)\} - uT\{U_P^D(x_{PM}) - U_N^D(x_{NM})\} \quad (18)$$

Observer II

Observer II is designed based on the Li-ion concentration dynamics given in (12) with the ‘measured’ information y_{pseudo} from the Observer I and voltage y_V . For this observer design, an Unscented Kalman Filter (UKF) is used to take care of the essential nonlinearity in the output functions. UKF is developed from the widely used Extended Kalman Filter (EKF) approach for nonlinear systems [26], [27]. UKF follows the same prediction-correction steps as EKF. However, instead of using the Jacobian as in EKF, UKF applies unscented transform. To apply the UKF approach in the present case, the Li-ion concentration dynamics in (12) is transformed into a discrete-time system using Euler’s discretization with sample time T_s . The resulting system takes the following form:

$$\begin{aligned} \begin{bmatrix} \bar{x}_P(k+1) \\ \bar{x}_N(k+1) \end{bmatrix} &= \begin{bmatrix} \bar{A}_P(k) & 0_M \\ 0_M & \bar{A}_N(k) \end{bmatrix} \begin{bmatrix} \bar{x}_P(k) \\ \bar{x}_N(k) \end{bmatrix} \\ &\quad + \begin{bmatrix} \bar{B}_P(k) \\ \bar{B}_N(k) \end{bmatrix} u(k) \\ Y(k) &= \begin{bmatrix} \bar{y}_V(k) \\ \bar{y}_{pseudo}(k) \end{bmatrix} = \begin{bmatrix} h_1(k, \bar{x}_P(k), \bar{x}_N(k), u(k)) \\ h_2(k, \bar{x}_P(k), \bar{x}_N(k), u(k)) \end{bmatrix} \end{aligned} \quad (19)$$

where \bar{x}_P and \bar{x}_N are discrete-time states, \bar{y}_V and \bar{y}_{pseudo} are the discrete-time outputs, $\bar{A}_P, \bar{A}_N, \bar{B}_P, \bar{B}_N$ are the time-varying matrices derived from the dynamic equations of (12) via discretization and h_1, h_2 are the time-varying functions derived from the output equations y_V in (12) and y_{pseudo} in (18). The system (19) can be written in compact form as:

$$\begin{aligned} x(k+1) &= A(k)x(k) + B(k)u(k) + q(k) \\ y(k) &= h(k, x(k), u(k)) + \bar{r}(k) \end{aligned} \quad (20)$$

where q represents the process noise accounting for the unmodeled dynamics and unknown disturbances; \bar{r} represents the measurement inaccuracies and unmodeled output uncertainties. The corresponding process and measurement noise covariance matrices are Q and R . The covariance of the state estimation is P_x . The UKF implementation follows the steps given below [27].

Step 1: Initial state $x(0)$, initial state covariance matrix $P_x(0)$ and noise covariance matrices Q and R are initialized.

Step 2: At time step k , a set of sigma points σ_i with $i = 1, \dots, 2M$ and some intermediate variables are generated as:

$$\begin{aligned} \chi_0(k-1) &= \hat{x}(k-1) \\ \chi_i(k-1) &= \hat{x}(k-1) + \sigma_i \\ \chi_{i+2M}(k-1) &= \hat{x}(k-1) - \sigma_i \end{aligned}$$

where $\hat{x}(k-1)$ is the estimated state from the time step $k-1$ and the sigma points are the columns of $\sqrt{2M\hat{P}(k-1)}$ with as estimated state covariance matrix from time step $k-1$.

Step 3: The intermediate variables are passed through the state dynamics as:

$$\chi_j(k/k-1) = A(k)\chi_j(k-1) + B(k)u(k), j = 0, \dots, 4M$$

Then the predicted state and covariance can be calculated as:

$$\begin{aligned}\hat{x}(k/k-1) &= \sum_{j=0}^{4M} W_j \chi_j(k/k-1) \\ \hat{P}_x(k/k-1) &= \sum_{j=0}^{4M} W_j \{ \chi_j(k/k-1) - \hat{x}(k/k-1) \} \{ \chi_j(k/k-1) \\ &\quad - \hat{x}(k/k-1) \}^T + Q\end{aligned}$$

where W_j are the weights.

Step 4: Now the estimated output, output covariance and cross covariance between state and output can be calculated as:

$$\begin{aligned}\hat{y}(k) &= h(k, \hat{x}(k/k-1), u(k)) \\ \gamma_j(k/k-1) &= h(k, \hat{x}(k/k-1), u(k)), j = 0, \dots, 4M \\ P_y(k/k-1) &= \sum_{j=0}^{4M} W_j \{ \gamma_j(k/k-1) - \hat{y}(k) \} \{ \gamma_j(k/k-1) - \hat{y}(k) \}^T + R \\ P_{xy}(k/k-1) &= \sum_{j=0}^{4M} W_j \{ \chi_j(k/k-1) - \hat{x}(k/k-1) \} \{ \gamma_j(k/k-1) - \hat{y}(k) \}^T\end{aligned}$$

Step 5: The filter gain is determined as:

$$L(k) = P_{xy}(k/k-1) \{ P_y(k/k-1) \}^{-1}$$

Then the state estimate and covariance are updated as:

$$\begin{aligned}\hat{x}(k) &= \hat{x}\left(\frac{k}{k}-1\right) + L(k) \{ y(k) - \hat{y}(k) \} \\ \hat{P}_x(k) &= \hat{P}_x(k/k-1) - L(k) P_y(k/k-1) L(k)^T\end{aligned}$$

where $y(k)$ is the measured output at time step k .

In the next time step $k+1$, the algorithm starts from *Step 2* again with $\hat{x}(k)$ and $\hat{P}_x(k)$ as initial state vector and covariance matrix, respectively.

Cell Capacity Estimation

In this part, the capacity estimation for the Li-ion cell is presented based on the estimated positive and negative electrode concentrations. Following the approach in [11], the total number of Li-ions contained in the cell can be computed as:

$$\begin{aligned}n_{Li} &= \frac{\varepsilon_s^+ L^+ A}{\frac{4}{3} \pi (R^+)^3} \int_0^{R^+} 4\pi r^2 c_s^+(r, t) dr \\ &\quad + \frac{\varepsilon_s^- L^- A}{\frac{4}{3} \pi (R^-)^3} \int_0^{R^-} 4\pi r^2 c_s^-(r, t) dr\end{aligned}\quad (21)$$

Using the above formula and the estimated node concentrations of positive and negative electrodes from

Observer II, the capacity of the cell can be estimated from the following:

$$\begin{aligned}\hat{n}_{Li} &= \frac{\varepsilon_s^+ L^+ A}{\frac{4}{3} \pi (R^+)^3} 4\pi \Delta_P^3 \sum_{i=1}^M i^2 \hat{c}_{sPi} \\ &\quad + \frac{\varepsilon_s^- L^- A}{\frac{4}{3} \pi (R^-)^3} 4\pi \Delta_N^3 \sum_{i=1}^M i^2 \hat{c}_{sNi}\end{aligned}\quad (22)$$

The estimate \hat{n}_{Li} serves as an indicator of the capacity of the Li-ion cell. The aging of the battery cell will eventually result in loss of cycle-able Li-ions and hence the value of the parameter n_{Li} will change correspondingly.

RESULTS & DISCUSSIONS

In this section, simulation studies are presented to verify the effectiveness of the estimation scheme. Battery cell model parameters of a 6.8 Ah LiCoO₂-Graphite cell are taken from [28]. To illustrate the state estimation performance, the surface concentration and bulk SOC (averaged concentration that is normalized against the maximum possible concentration in the electrodes) of individual electrodes are considered. An SPM model with correct initial condition is used as plant. The observer is designed based on the simplified SPM ODE approximation and initialized with different initial conditions than the plant. We present a constant IC current discharge scenario and the results are shown in Fig. 4 through Fig. 7. The estimated variables are initialized with different initial conditions. To emulate realistic scenario, the measured variables from the plant model are injected with zero mean Gaussian noise 1 mV, 1 mA and 0.1°C. It can be seen from the results that the estimation scheme performs reasonably and is able to estimate the variables with good accuracy. Further, a decreasing capacity scenario is shown in Fig. 8 which indicates that the scheme is able to track the decreasing capacity.

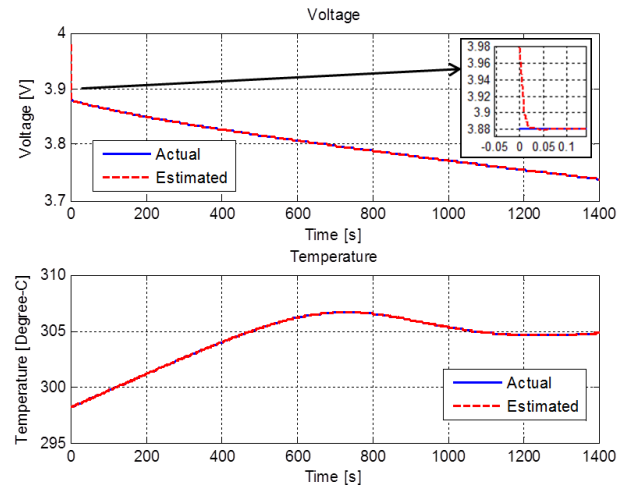


Figure 4: Voltage and temperature estimation performance

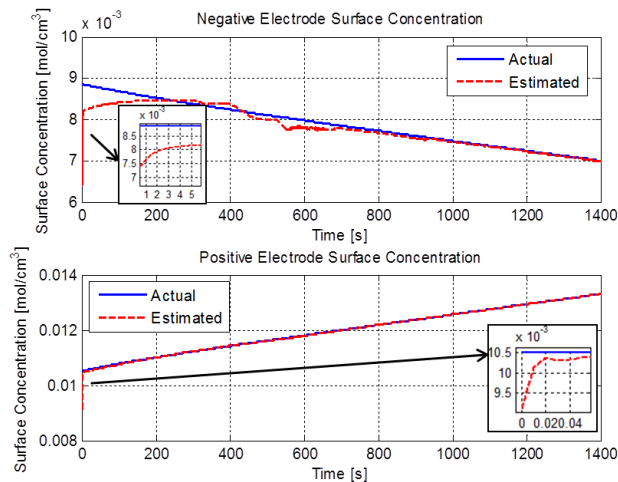


Figure 5: Surface concentration estimation performance

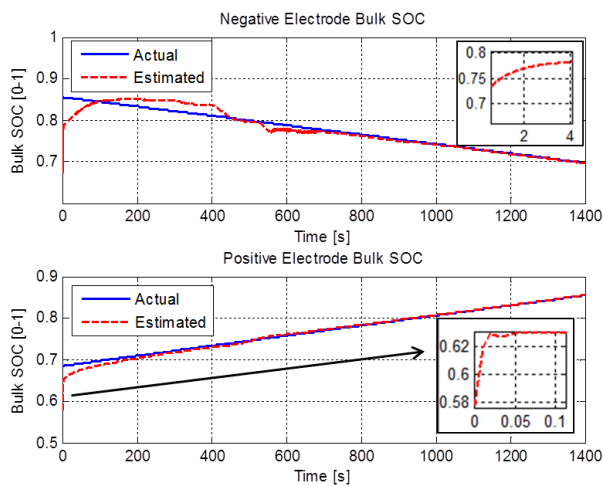


Figure 6: Negative and positive electrode bulk SOC estimation performance

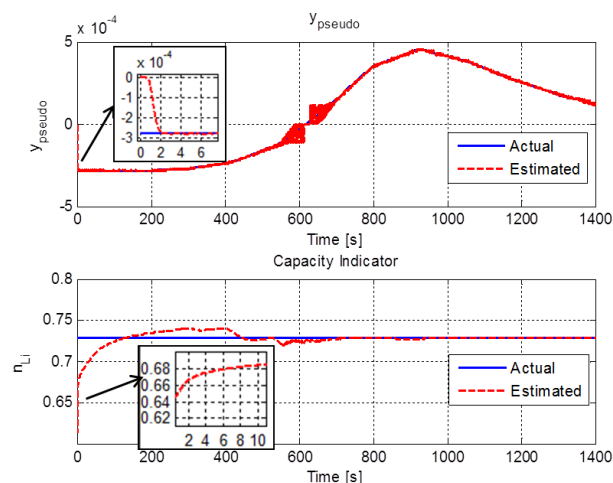


Figure 7: Pseudo-measurement and capacity estimation performance

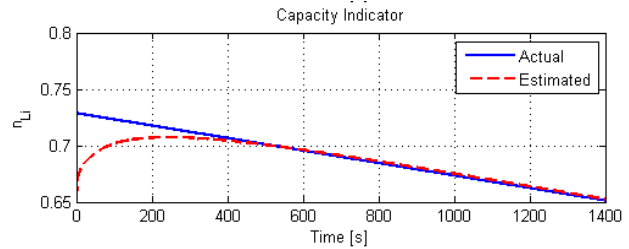


Figure 8: Tracking of decreasing capacity

CONCLUSION

In this paper, an estimation scheme is presented for estimation of Li-ion concentrations in both the negative and positive electrodes of the Li-ion cell. We adopt the two-electrode SPM coupled with averaged lumped thermal dynamics and show that the Li-ion concentration states of both electrodes are observable from the measurable temperature and voltage. Then, we proposed an estimation scheme consisting of two observers working in cascade. The first observer essentially estimates the Li-ion concentration information from the thermal model and the measured temperature. The second observer uses this information along with the measured voltage and in turn estimates the Li-ion concentration states of both electrodes. The effectiveness of the observer is verified by simulation studies.

However, there are some aspects that should be explored as future work of this study. First, the scheme is illustrated using particular battery chemistry (LiCoO₂-Graphite). The effectiveness of the scheme should be explored for other chemistries. Second, the scheme is based on conventional SPM model coupled to averaged lumped thermal dynamics. The proposed scheme cannot be readily applied to the enhanced models [22], [23]. Next, solutions should be investigated to deal with the sensitivity to high noise levels in the measurements.

ACKNOWLEDGMENTS

This research is supported, in part, by the US Department of Energy GATE program under grant number DE-EE0005571 and NSF under grant number CMMI-1055254.

REFERENCES

- [1] Saha, B., Goebel, K., Poll, S., and Christophersen, J., 2007. "An integrated approach to battery health monitoring using bayesian regression and state estimation". In 2007 IEEE Autotestcon, pp. 646-653.
- [2] Ng, K. S., Moo, C., Chen, Y., and Hsieh, Y., 2009. "Enhanced coulomb counting method for estimating state-of-charge and state-of-health of lithium-ion batteries". *Applied Energy*, vol. 86, no. 9, pp. 1506-1511.
- [3] Plett, G. L., 2004. "Extended Kalman filtering for battery management systems of LiPB-based HEV battery packs: Part 3. State and parameter estimation". *Journal of Power sources*, vol. 134, no. 2, pp. 277-292.
- [4] Kim, Il-Song, 2010. "A Technique for Estimating the State of Health of Lithium Batteries Through a Dual-

- Sliding-Mode Observer”. *IEEE Transactions on Power Electronics*, vol.25, no.4, pp.1013-1022.
- [5] Chaturvedi, N. A., Klein, R., Christensen, J., Ahmed, J., and Kojic, A., 2010. “Algorithms for Advanced Battery-Management Systems”. *IEEE Control Systems Magazine*, vol.30, no.3, pp.49-68.
- [6] Doyle, M., Fuller, T. F., and Newman, J., 1993. “Modeling of galvanostatic charge and discharge of the lithium/polymer/insertion cell”. *Journal of the Electrochemical Society*, vol. 140, no. 6, pp. 1526-1533.
- [7] Smith, K. A., Rahn, C. D., and Wang, C., 2010. “Model-based electrochemical estimation and constraint management for pulse operation of lithium ion batteries”. *IEEE Transactions on Control Systems Technology*, vol. 18, no. 3, pp. 654-663.
- [8] Klein, R.; Chaturvedi, N.A.; Christensen, J.; Ahmed, J.; Findeisen, R.; Kojic, A., 2013. “Electrochemical Model Based Observer Design for a Lithium-Ion Battery”. *IEEE Transactions on Control Systems Technology*, vol.21, no. 2, pp. 289-301.
- [9] Santhanagopalan, S., and White, R. E., 2006. “Online estimation of the state of charge of a lithium ion cell”. *Journal of Power Sources*, vol. 161, no. 2, pp. 1346-1355.
- [10] Domenico, D., Stefanopoulou, A., and Fiengo, G., 2010. “Lithium-ion battery state of charge and critical surface charge estimation using an electrochemical model-based extended Kalman filter”. *ASME Journal of Dynamic Systems, Measurement, and Control*, vol. 132, no. 6, pp. 061302.
- [11] Moura, S. J., Chaturvedi, N. A., and Krstic, M., 2012. “PDE estimation techniques for advanced battery management systems—Part I: SOC estimation”. In 2012 American Control Conference (ACC), pp. 559-565.
- [12] Dey, S., and Ayalew, B., “Nonlinear Observer Designs for State-of-Charge Estimation of Lithium-ion Batteries”. In 2014 American Control Conference (ACC), pp.248-253.
- [13] Dey, S., Ayalew, B., and Pisu, P., 2014. “Nonlinear Robust Observers for State-of-Charge Estimation of Lithium-ion Cells Based on a Reduced Electrochemical Model”. *IEEE Transactions on Control System Technology*, available online, DOI: 10.1109/TCST.2014.2382635.
- [14] Samadi, M. F., Alavi, S. M., and Saif, M., 2013. “Online state and parameter estimation of the Li-ion battery in a Bayesian framework”. In 2013 American Control Conference (ACC), pp. 4693-4698.
- [15] Schmidt, A. P., Bitzer, M., Imre, Á. W., and Guzzella, L., 2010. “Model-based distinction and quantification of capacity loss and rate capability fade in Li-ion batteries”. *Journal of Power Sources*, vol. 195, no. 22, pp. 7634-7638.
- [16] Fang, H., Wang, Y., Sahinoglu, Z., Wada, T., and Hara, S., 2014. “State of charge estimation for lithium-ion batteries: An adaptive approach”. *Control Engineering Practice*, vol. 25, pp. 45-54.
- [17] Moura, S. J., Chaturvedi, N. A., and Krstic, M., 2013. “Adaptive PDE Observer for Battery SOC/SOH Estimation via an Electrochemical Model”. *ASME Journal of Dynamic Systems, Measurement, and Control*, vol. 136, no. 1.
- [18] Wang, Y., Fang, H., Sahinoglu, Z., Wada, T. and Hara, S., 2014. “Adaptive Estimation of the State of Charge for Lithium-Ion Batteries: Nonlinear Geometric Observer Approach,” In *IEEE Transactions on Control Systems Technology*, available online.
- [19] Dey, S., Ayalew, B., and Pisu, P., 2014. “Combined estimation of State-of-Charge and State-of-Health of Li-ion battery cells using SMO on electrochemical model.” In 13th International Workshop on Variable Structure Systems, Nantes, France, June 29-July 2, pp. 1-6.
- [20] Dey, S., Ayalew, B., and Pisu, P., 2014. “Adaptive Observer Design for a Li-Ion Cell Based on Coupled Electrochemical-Thermal Model.” In *ASME 2014 Dynamic Systems and Control Conference*.
- [21] Guo, M., Sikha, G., and White, R.E., 2011. “Single-particle model for a lithium-ion cell: thermal behavior”. *Journal of The Electrochemical Society*, vol. 158, no. 2, pp. A122-A132.
- [22] Tanim, T. R., Rahn, C. D., and Wang, C. Y., 2014. “A Temperature Dependent, Single Particle, Lithium Ion Cell Model Including Electrolyte Diffusion,” In *ASME Journal of Dynamic Systems, Measurement, and Control*.
- [23] Lin, X., Perez, H. E., Siegel, J. B., Stefanopoulou, A. G., Li, Y., Anderson R. D., Ding, Y., and Castanier, M. P., 2013. “Online Parameterization of Lumped Thermal Dynamics in Cylindrical Lithium Ion Batteries for Core Temperature Estimation and Health Monitoring”. *IEEE Transactions on Control Systems Technology*, vol.21, no.5, pp.1745-55.
- [24] Hermann, R., and Krener, A, 1977. “Nonlinear Controllability and Observability,” In *IEEE Transactions on Automatic Control*, vol. 22, no. 5, pp. 728-740, 1977.
- [25] Utkin, V., Guldner, J., and Shi, J., 1999. *Sliding mode control in electromechanical systems*. CRC press.
- [26] Julier, S. J., and Uhlmann, J. K., 1996. “A general method for approximating nonlinear transformations of probability distributions.” Robotics Research Group, Department of Engineering Science, University of Oxford, UK, Technical Report, 1996.
- [27] Xiong, K., Zhang, H., and Chan, C., 2006. “Performance evaluation of UKF-based nonlinear filtering,” In *Automatica*, vol. 42, no. 2, pp. 261-270.
- [28] Speltino, C., Domenico, D. Di, Stefanopoulou, A., and Fiengo, G., 2009. “Experimental identification and validation of an electrochemical model of a lithium-ion battery.” In *Proceedings of 2009 IEEE European Control Conference*.